

# Gliding Movement of and Bidirectional Transport along Single Native Microtubules from Squid Axoplasm: Evidence for an Active Role of Microtubules in Cytoplasmic Transport

ROBERT DAY ALLEN,<sup>\*\*</sup> DIETER G. WEISS,<sup>\*§</sup> JOHN H. HAYDEN,<sup>\*\*||</sup>  
DOUGLAS T. BROWN,<sup>\*||</sup> HIDESHI FUJIWAKE,<sup>\* \*\*</sup> and MARCIA SIMPSON<sup>\*\*\*</sup>

<sup>\*</sup>Marine Biological Laboratory, Woods Hole, Massachusetts 02543; <sup>\*</sup>Department of Biology, Dartmouth College, Hanover, New Hampshire 03755; and <sup>§</sup>Zoologisches Institut, Universität München, D-8000 München 2, Federal Republic of Germany. Present Address: <sup>||</sup>Department of Biology, Siena College, Loudonville, New York 12211; <sup>§</sup>Dartmouth Medical School, Hanover, New Hampshire 03755; <sup>\*\*</sup>Hamamatsu Phototonics K.K., Hamamatsu City, Japan; <sup>\*\*</sup>Amherst College, Amherst, Massachusetts 01002.

**ABSTRACT** Native microtubules prepared from extruded and dissociated axoplasm have been observed to transport organelles and vesicles unidirectionally in fresh preparations and more slowly and bidirectionally in older preparations. Both endogenous and exogenous (fluorescent polystyrene) particles in rapid Brownian motion alight on and adhere to microtubules and are transported along them. Particles can switch from one intersecting microtubule to another and move in either direction. Microtubular segments 1 to 30  $\mu\text{m}$  long, produced by gentle homogenization, glide over glass surfaces for hundreds of micrometers in straight lines unless acted upon by obstacles. While gliding they transport particles either in the same (forward) direction and/or in the backward direction. Particle movement and gliding of microtubule segments require ATP and are insensitive to taxol (30  $\mu\text{M}$ ). It appears, therefore, that the mechanisms producing the motive force are very closely associated with the native microtubule itself or with its associated proteins.

Although these movements appear irreconcilable with several current theories of fast axoplasmic transport, in this article we propose two models that might explain the observed phenomena and, by extension, the process of fast axoplasmic transport itself. The findings presented and the possible mechanisms proposed for fast axoplasmic transport have potential applications across the spectrum of microtubule-based motility processes.

Fast axoplasmic transport is one of a number of fundamental cellular motility processes for which the mechanism is not known in detail, yet microtubules clearly play an integral and possibly fundamental role (for reviews see references 30, 50, 51, 62, 70, 71, 73). The most intriguing question about the involvement of microtubules is whether their role is only passive, serving as guide elements or tracks for some other force-generating system, or whether they might be involved directly in force generation. Although many hypotheses of axoplasmic transport propose a passive role for microtubules

(52, 67), some models suggest that microtubules or their associated proteins may be involved in the force production or contain the force-generating enzymes (31, 37, 50).

Some authors have suggested a role in axoplasmic transport for actin and myosin (17, 29, 42, 44), but most of the recent evidence does not favor an actomyosin mechanism of force generation (16, 25, 26, 28, 71).

The giant axon of the squid *Loligo pealei* was selected as material for the present study not only because of the volume of axoplasm that can be obtained from a single axon (5 to 10

$\mu\text{l}$ ), but also because transport of organelles and vesicles (particles) continues in the extruded axoplasm for several hours, as long as ATP is available as a source of energy (15). Our strategy, a more direct approach to motile processes, is based on the results of high resolution video-enhanced microscopy supported by electron microscopy where necessary, rather than on ultrastructural research alone. The Allen video-enhanced contrast (AVEC)<sup>1</sup> method of videomicroscopy (3–5, 8) developed during the last few years makes it possible to detect, visualize, and analyze the motile behavior of small organelles and cytoskeletal elements (34, 35).

In the course of earlier work it was observed that “filaments” of unknown identity often protruded from the axoplasmic surface into the buffer and transported particles (15). In a progress report given at the Marine Biological Laboratory in 1983 it was shown for the first time by some of the authors (6) that “motile filaments” could be dissociated from extruded axoplasm and that some of these transported particles unidirectionally, whereas others transported bidirectionally. In this report there were also indications that the filaments themselves might be motile.

We now report the results of our continuing studies of the identity and ultrastructure of these filaments, and the results of our recent attempt to explore and quantify the full range of their motile capabilities. We present evidence that the filaments separated from squid axoplasm are native microtubules and that they themselves can glide over glass surfaces and transport organelles and vesicles. These previously unknown properties of native microtubules enable us to present much more detailed and testable hypotheses for the mechanisms that may underlie microtubule-dependent motility in the axon and a number of other cellular processes of fundamental biomedical importance.

## MATERIALS AND METHODS

**Materials:** Freshly collected squid (*Loligo pealei*) from 12 to 20 cm in body length were obtained daily from the Department of Marine Resources of the Marine Biological Laboratory (Woods Hole, MA). Giant axons were dissected (27), washed several times in  $\text{Ca}^{++}$ -free sea water, and extruded (13) into 50  $\mu\text{l}$  of axoplasmic dissociation buffer of the following composition (expressed as millimolar): 200  $\text{K}^+$  aspartate, 37 taurine, 20 betain, 15 glycine, 8 HEPES, 3.7  $\text{MgCl}_2$ , 2.8  $\text{K}^+$ -EGTA, 0.86  $\text{CaCl}_2$ , 0.3 D-glucose, <1 to 20  $\text{K}^+$ -ATP,  $10^{-6}$  M phenylmethylsulfonyl fluoride, pH 7.2. This is similar to Buffer-X in reference 16 but more dilute. All experiments were performed at a room temperature of 21°C.

The axoplasm in dissociation buffer was placed on a 24 × 50 mm No. 0 cover glass supported by a stainless steel frame and covered by a smaller cover glass, usually 22 × 22 mm (No. 1). Observations were made over 2–8-h periods on preparations sealed or partially sealed with Valap (Vaseline, lanolin, paraffin 1:1:1).

We obtained motile microtubule segments by homogenizing the extruded axoplasm in 40  $\mu\text{l}$  of dissociation buffer in a homemade Dounce-type homogenizer (inner diameter 2.0 mm) with a loosely fitting pestle. Four or five gentle strokes were sufficient to fragment the microtubules into segments 0.5–30  $\mu\text{m}$  long.

In some experiments we added taxol to the dissociation buffer (30  $\mu\text{M}$  final concentration). In other experiments, fluorescent latex beads (570 nm diam; Polysciences Inc., Warrington, PA) were applied to the preparation in the same buffer.

In experiments with motile microtubule fragments, cover glasses were used untreated or treated experimentally by the following procedures: (a) silicization (Prosil-28; PCR Research Chemicals, Inc., Gainesville, FL); (b) detergent wash followed by rinsing in distilled deionized water; (c) detergent wash followed by rinsing in absolute ethanol and subsequent flaming; (d) coating with poly-L-ornithine (110,000 or 15,000 mol wt) or poly-L-lysine (800,000

mol wt); or (e) coating with poly-L-ornithine (15,000 mol wt), then with doubly concentrated poly-L-aspartate (15,000 to 20,000 mol wt).

All poly-amino acids were obtained from Sigma Chemical Co. (St. Louis, MO) and applied according to Collins (20).

**Methods:** The motile behavior of the dissociated axoplasm was observed by AVEC-differential interference contrast videomicroscopy (3–5, 8). The internally corrected 100× planapochromatic oil immersion objective of the inverted Zeiss Axiomat microscope equipped with a 50 W mercury arc lamp was used, yielding a magnification on the TV monitor (screen width 25 cm) of 10,000×. Real time analogue video enhancement and digital image processing with the Hamamatsu C 1966 Photonic Microscope System (Photonic Microscopy Inc., Oak Brook, IL) consisted of the following steps: (a) AVEC analogue enhancement of the full aperture image at an instrumental compensator setting of  $\lambda/9$ , with gain and offset adjusted to from about one-third to one-half of their respective ranges; (b) digital subtraction of the fixed pattern of mottle that is an inevitable consequence of analogue enhancement; (c) in some cases, reduction of pixel noise by a real-time digital rolling average operation over two or four frames; (d) manipulation of the gray scale by stretching of the pixel brightness histogram.

To demonstrate movements of long microtubules in tangles, autosubtraction with the specimen in focus was carried out to show changes in microtubular position and loop diameter. In this mode, the image initially disappeared then gradually reappeared, showing only moving structures and their original positions in reverse contrast.

Fluorescent particles were detected with a Hamamatsu C 1000-12 silicon-intensified target (SIT)-camera head connected to the C 1966 image processor. These particles were analyzed quantitatively with the trace function of the C 1966; the Hamamatsu C 1055 x, y-tracker, or the Hamamatsu C 2117 video manipulator (Photonic Microscopy Inc.).

Video-enhanced microscope images were recorded simultaneously in real time by a normal speed video cassette recorder (Sony model VO-5800 or VO-2600; Sony Corp. of America, Long Island City, NY) and by a time lapse recorder (Sony model TV0-9000, no longer commercially available in the United States) for display at an acceleration of 10 times.

Video analysis was carried out in several ways. Preliminary velocity analysis was done by a computer method described previously (7). Detailed analyses were performed with the Hamamatsu model C 2117 video manipulator, which permits single particles or microtubule segments to be analyzed with respect to both trajectory and instantaneous velocity history.

We performed electron microscopy by placing several Formvar- and carbon-coated gold finder grids in the dissociated preparations. Either the grids were removed after the observation and stained with 0.5% uranyl acetate for negative staining according to Langford (45) or the preparation was fixed by perfusion with 1% glutaraldehyde in 0.1 M cacodylate buffer of pH 7.4 and stained with 0.5% uranyl acetate for whole mount electron microscopy (74). Aliquots of homogenized preparations were processed for negative staining as described by Langford (45).

Electron microscopy was performed with a JEOL 100CX electron microscope with stereo attachments. A 60- $\mu\text{m}$  aperture was used for negative stain, and an aperture of 40  $\mu\text{m}$  for whole-mounts. The microscope was operated at an accelerating voltage of 80 kV.

## RESULTS

### *Transport of Organelles and Vesicles along “Filaments” Continued during Gradual Dissociation of the Axoplasm*

Incubation of extruded squid axoplasm in the dissociation buffer caused a gradual dissociation of the axoplasm into a more or less tangled mass of “filaments” which served as substrata (or “tracks”) for the transport of organelles and vesicles (collectively called “particles”) (Fig. 1). The vesicles are of very low contrast and by the criteria of size and abundance correspond to the many synaptic vesicles visible in intact axon (7, 38).

There were several typical stages or conditions of the dissociation process that were distinguishable. Not every stage was seen in every preparation. In all of these, continuous movement along the filaments was observed:

**STAGE 1. AXOPLASMIC CYLINDER:** The extruded cylinder of axoplasm retains its highly ordered parallel arrangement of filaments in its interior. The morphology and motility

<sup>1</sup> Abbreviation used in this paper: AVEC, Allen video-enhanced contrast.

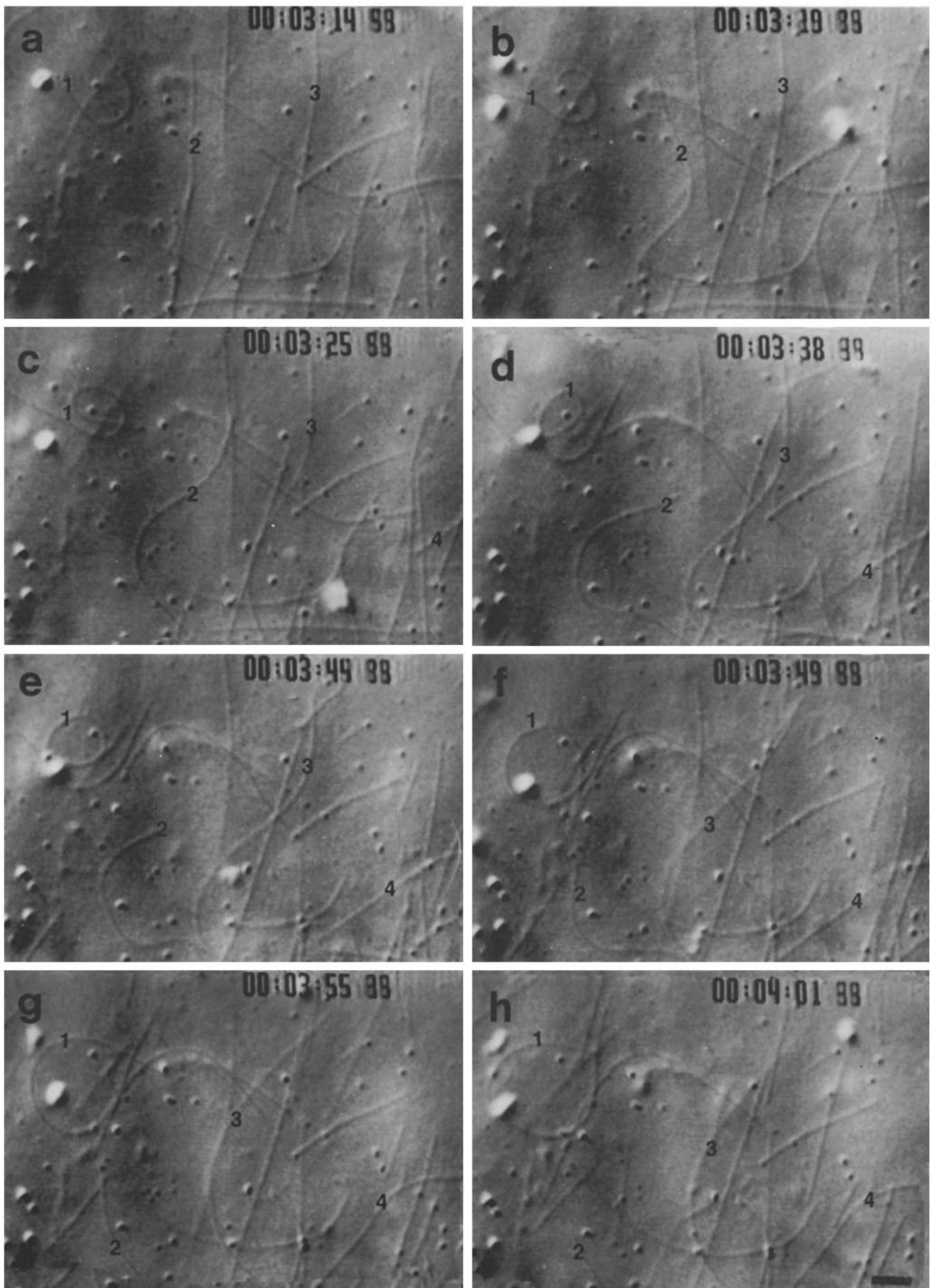


FIGURE 1 A sequence of videomicrographs (0.5-exposure) at times indicated over a period of 46 s shows that almost all long microtubules undergo changes in position and shape. The four most evident long microtubules with shape changes are indicated by numbers. Timer indicates hours, minutes, seconds, and hundredths of a second. Bar, 2  $\mu$ m.  $\times$  4,000.

of its interior are qualitatively indistinguishable from those of intact axons (15, 16).

**STAGE 2. SURFACE OF THE AXOPLASMIC CYLINDER:** The surface of the axoplasmic cylinder adjacent to the cover glass shows the individual filaments in disorder, somewhat loosened, curly, and frequently intersecting. Vesicles and larger organelles move along individual filaments rapidly and almost unidirectionally.

**STAGE 3. PROTRUDING FILAMENTS:** With time the free ends of filaments, which continue to move particles, protrude from the free surface of the axoplasmic cylinder. This is one source of the numerous particles that are released from the bulk axoplasm and remain in Brownian motion in the medium surrounding the filaments. The filaments wave gently, probably actively as well as by Brownian motion. They have the appearance of seaweed waving under water.

**STAGE 4. SEPARATE FILAMENTOUS TANGLES:** Sometimes filamentous tangles can be found at a variable distance from the axoplasm proper. With time, apparently more and more filaments fall free or move a certain distance from the axoplasm. Both axial and lateral movements have been observed (Fig. 1). Filaments are found on the surface of the lower cover glass where they continue to be in motion and/or to move particles that have alighted upon them from the surrounding medium (Fig. 1).

**STAGE 5. ASTERLIKE ARRAYS:** In some cases these tangled masses form loose knots or asterlike arrays with filaments transporting particles in and out of a center where the particles tend to accumulate (Fig. 2).

**STAGE 6. FREE FILAMENT FRAGMENTS:** Sometimes short segments of the filaments come free from the tangles or from the axoplasm proper and glide over the glass surface. The number of fragments can be increased by gentle homogenization so that a field 25  $\mu\text{m}$  wide with a depth of focus of  $\sim 0.3 \mu\text{m}$  may contain up to 100 filaments, most of which show the gliding motion, and many of them simultaneously transport particles in one or both directions (Fig. 3). Particles moving forward along gliding microtubules often accumulated at the end, forming a knob resembling the head of a cane.

**STAGE 7. AGED PREPARATIONS:** After 1 h—earlier in the cases where ATP was only 1.0 mM—the movement of the particles slowed down considerably concomitant with the

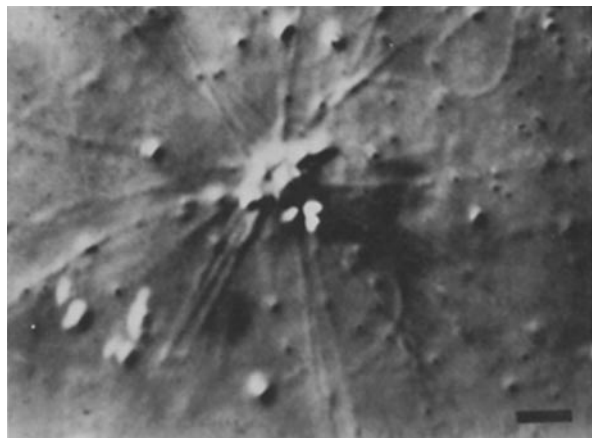


FIGURE 2 A tangle or knot to long microtubules, each of which was transporting particles unidirectionally either toward or away from the center. Bar, 2  $\mu\text{m}$ .  $\times 3,500$ .

speed of filament gliding, and bidirectionality of transport on individual filaments became more pronounced.

**STAGE 8. TERMINAL STAGE:** After several hours, when only Brownian motion persisted, many particles were found attached all along the filaments. Some of them appeared to be bound to the filaments by some kind of microscopically unresolved filament with a length of up to 0.5  $\mu\text{m}$  showing apparent “tethered Brownian motion.”

### Ultrastructure

Electron micrographs of negatively stained filaments with particles attached clearly showed that these were actually native microtubules, almost all of them single. In some preparations particles were found to be attached by thin bridging filaments of irregular appearance and unknown molecular identity. The microtubules themselves were surrounded by an amorphous “fuzzy coat” which sometimes resembled a loose helix (Fig. 4).

The particle-laden microtubules do not appear to be associated with other recognizable cytoskeletal elements, at least not in any apparent functional relationship. That is not to say, however, that the preparations are devoid of other filamentous structures. Filaments the size of neurofilaments, which are very numerous in intact axoplasm (38), are frequently seen in these preparations and are more numerous than microtubules. However, they rarely show associated vesicles and have a much more curly appearance, whereas only the microtubules in the electron micrographs appear as straight as the filaments seen by light microscopy.

### Details of Particle Movements

Particles in suspension around the filaments were in vigorous Brownian motion, but once they came close to or collided with the filaments, they adhered to them and were transported. Movement of small particles rarely stopped before they reached the end of the microtubule. Larger organelles sometimes stopped for a while and continued to move within seconds or minutes, but real stops or “jamming” were not often observed except when two or more microtubules intersect. These particles only rarely became detached along the filament length and in most cases remained attached until they came to the end of the filament. There, one or a few particles occasionally remained at the end of a filament, as was seen predominantly in older preparations and on microtubular fragments (see below).

In preparations that were either fresh and/or contained  $>1.0 \text{ mM}$  exogenous ATP, the movements of particles along the vast majority of microtubules appeared to be unidirectional. In these preparations, speeds reached 2  $\mu\text{m/s}$ , almost as fast as in the intact axon.

The vesicles (smallest particles) moved continuously without interruption or changes of direction, just as in the intact cell. The movements of large organelles were neither so rapid nor so regular, although some moved as rapidly as vesicles. In fresh preparations or ones containing at least 1.0 mM ATP the movement was fastest, and the tendency to unidirectional transport was more pervasive. The density of traffic appears to depend on the concentration of particles in suspension, which varies considerably with time and distance from the axoplasm.

As preparations were observed over time, the velocity of

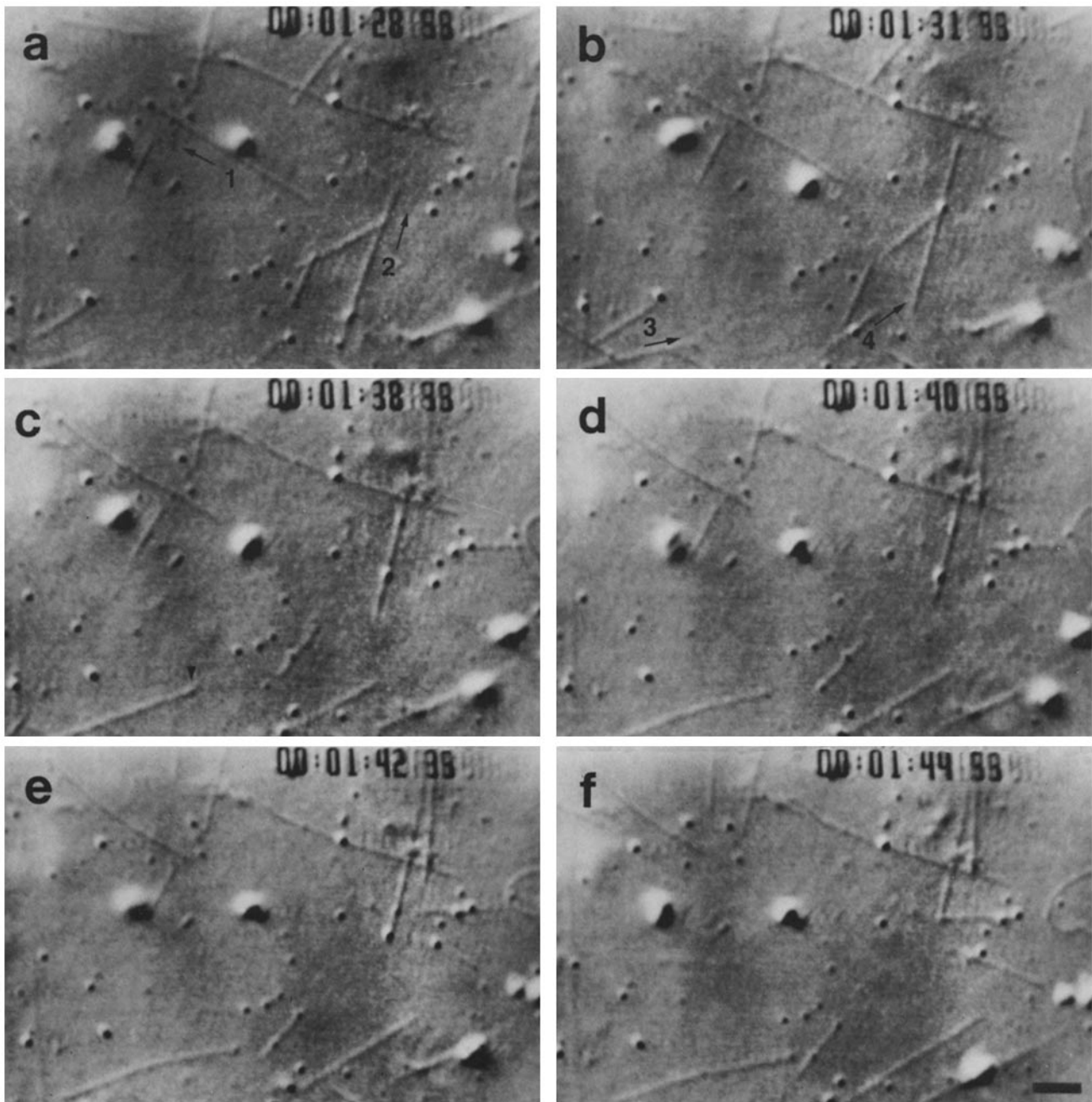


FIGURE 3 A sequence of videomicrographs at the times shown depicts the gliding of four filament fragments over a period of 17 s. Arrows show the directions of gliding. Two fragments became detached and were carried out of the plane of focus by Brownian motion. Arrowhead shows particles carried at the frontal end of a gliding microtubule. Bar, 2  $\mu\text{m}$ .  $\times$  4,000.

particle movement decreased, while the incidence of bidirectional transport increased (Table I). In some preparations, bidirectional transport became the dominant mode, in which the larger particles moved more slowly and predominantly in the direction opposite the transport of the small vesicles (Table I).

Vesicles and small particles are the most numerous and move most rapidly in one direction, which probably corresponds to the orthograde direction, since this compares well with the situation in intact axons. In cases where similar numbers of particles move in either direction the movement is not symmetrical: large particles move more frequently in

what would correspond to the retrograde direction and do so with decreasing speed as their size increases. The velocity of orthograde particles in contrast seems to be almost independent of size (Table I).

Particles traveling in opposite directions along the same microtubule usually do not interact in such a way as to perturb their respective movement or velocity when they pass one another (Fig. 5). Only in some cases do two particles collide and then one may leave the microtubule. In many scenes the large particles appear to be more loosely attached to the microtubules and seem to be hopping over the small ones.

When two microtubules that are not parallel cross one



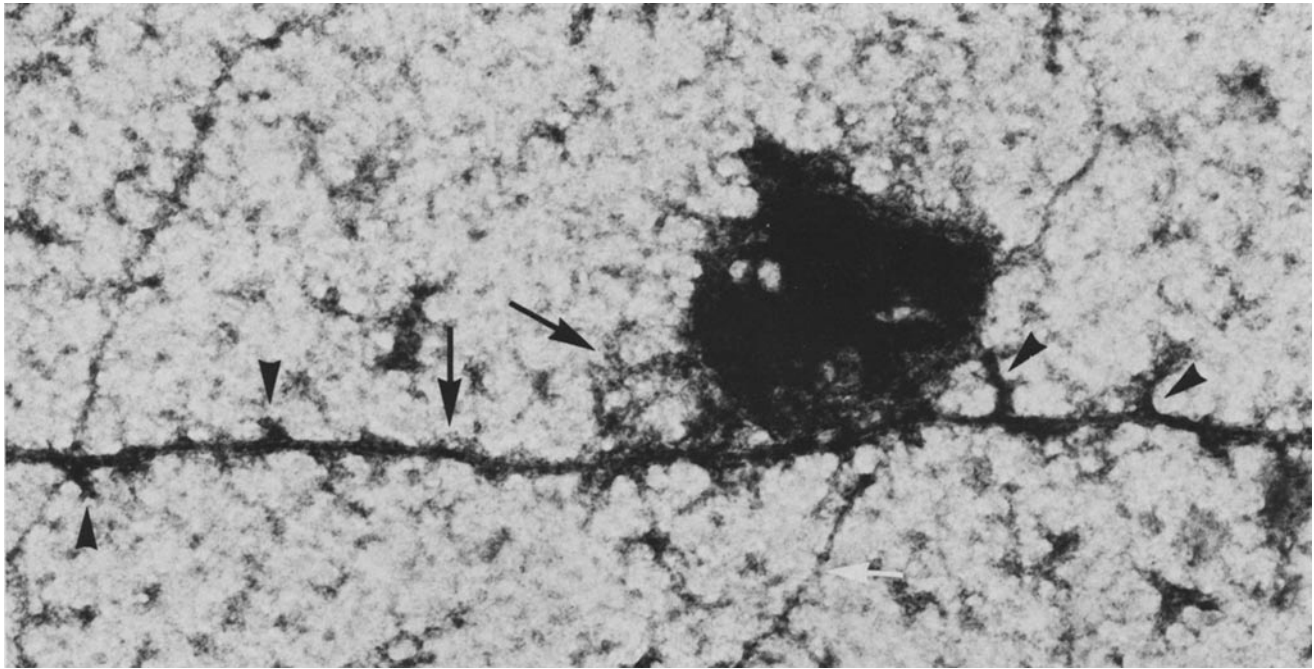


FIGURE 4 Electron micrograph of a negatively stained native microtubule with an associated large particle. Also present is an amorphous, possibly helical fuzzy coat around part of the microtubule (arrow). Similar material is around the particle (arrow). The microtubule surface also has a few projections (arrowheads). Neurofilaments were also observed (white arrow).  $\times 68,340$ .

another, particles moving along one of them may switch to the other and move in either direction along it without an apparent pause or change of speed (Fig. 5). Simultaneous attachment of a particle to two neighboring or intersecting microtubules can cause the microtubules to become deformed under stress. When one microtubule becomes detached from the particle, both microtubules recoil elastically (Fig. 5).

The speed at which particles moved varied from one preparation to another and depended on the concentration of ATP available. We repeatedly observed that the addition of ATP to preparations in which transport had slowed down increased the speed of the particles several fold, but the speed never reached that observed in intact axons.

In preliminary experiments, fluorescent polystyrene particles  $0.537 \mu\text{m}$  in diameter were added to an active preparation and their movement was recorded immediately. Although in the fluorescence mode the microtubules could not be seen, it was clear that some particles did not show the characteristic Brownian motion and were transported linearly and in the same manner as the organelles and vesicles. The speed was estimated to be  $0.135 \pm 0.005 \mu\text{m/s}$ , which corresponds well to the speed of large particles moving retrogradely (compare Table I).

### *Movements of Microtubules*

Long ( $>30 \mu\text{m}$ ) segments of microtubules within the filamentous tangles near the edges of the extruded axoplasm became deformed irrespective of whether particles were transported along them or not. This could best be demonstrated by autosubtraction with the image processor. These images initially lacked contrast except for that due to structures that had moved. It was clear from Fig. 1 that microtubular loops changed not only their shape and position but also their radius of curvature from the initiation of autosubtraction. The free

ends of microtubules protruding from tangles or from the surface of bulk axoplasm showed graceful waving and sometimes serpentine movement. These movements are ATP dependent and can be clearly distinguished from Brownian motion. The latter is responsible for a more rapid oscillation of small amplitude and is characteristic of preparations in which all motility has ceased.

When two microtubules intersected, one was frequently bent by the other, as if pulled or stroked in some manner. This could be attributed in almost all cases to a moving particle contacting or transiently attaching to the transverse filament (Fig. 5). Particles seem to have multiple "binding sites" (compare reference 48) since often a particle moving along one microtubule pulls another microtubule with it. Attachment to more than one microtubule is most often seen with large spherical particles and mitochondria but may also occur with the particles of the smallest size class.

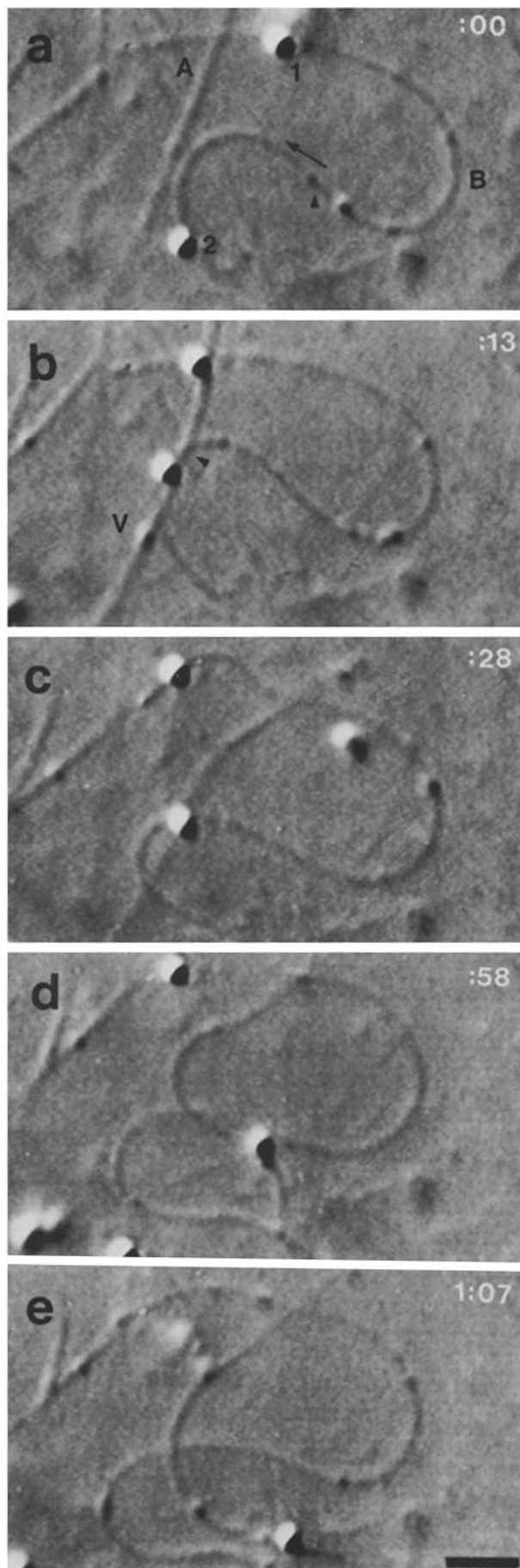
Shorter segments (1 to  $30 \mu\text{m}$ ) of microtubules obtained by gentle homogenization of extruded axoplasm glide over the glass surface at velocities between  $0.1$  and  $0.7 \mu\text{m/s}$  (Table II, Figs. 9 and 13). The gliding of individual microtubules is strictly unidirectional. Individual microtubules can glide in any direction through the field of observation and usually follow almost straight paths (Figs. 3 and 6). The paths of gliding microtubules are all different and cannot be attributed to tracks on the glass surface or to streaming of the medium in the preparation. For the most part, they did not deform or change direction unless interacting with particles attached to glass. In such cases microtubules usually detached from the glass surface and disappeared out of the focus or changed direction while remaining stiff all of the time (e.g., Fig. 3 and 86 in Fig. 6).

When a gliding microtubule was completely stopped by colliding with a particle stuck to the glass, it was blocked from

TABLE I  
Particle Movement Among Individual Microtubules Attached to Glass

Microtubule No. (series)	A1	A2	A3	A4	A5	B1	B2	B3
Age of preparation at start of evaluation (min)	15	15	15	45	75	200	200	200
Total number of particles counted	158	220	156	417	182	193	81	79
Orthograde particles/min	22.4 ± 7.4 (7)	30.7 ± 6.4 (7)	25.8 ± 6.2 (6)	27.2 ± 6.0 (15)	28.5 ± 8.1 (6)	4.6 ± 2.3 (16)	3.1 ± 1.9 (16)	2.4 ± 1.2 (16)
Retrograde particles/min	0.14 ± 0.35 (7)	0.71 ± 0.70 (7)	0.17 ± 0.37 (6)	0.6 ± 0.9 (15)	1.8 ± 1.1 (6)	7.4 ± 2.8 (16)	2.1 ± 1.3 (16)	2.6 ± 0.60 (16)
Percentage of orthograde particles								
Size class								
Small	99.4 (157)	97.7 (213)	99.4 (155)	98.2 (270)	92.4 (97)	37.9 (58)	62.5 (30)	50.0 (31)
Medium	None	None	None	97.0 (130)	97.2 (70)	51.7 (15)	65.2 (15)	63.6 (7)
Large	None	100 (2)	None	100 (8)	80.0 (4)	9.1 (1)	30.0 (3)	None
All particles	99.4 (157)	97.7 (215)	99.4 (155)	97.8 (408)	94.0 (171)	38.3 (74)	59.3 (48)	48.1 (38)
Orthograde velocity (μm/s)								
Size class								
Small	1.8 ± 0.15 (19)	1.72 ± 0.18 (22)	1.51 ± 0.23 (22)	1.29 ± 0.16 (6)	1.36 ± 0.13 (3)	0.75 (2)	0.74 (1)	0.47 ± 0.13 (7)
Medium	None	None	None	1.19 ± 0.41 (6)	1.12 ± 0.15 (14)	0.82 ± 0.21 (3)	0.66 ± 0.25 (5)	0.52 ± 0.18 (6)
Large	None	None	None	None	1.12 (1)	None	0.73 ± 0.11 (3)	None
All particles	1.8 ± 0.15 (19)	1.72 ± 0.18 (22)	1.51 ± 0.23 (22)	1.24 ± 0.29 (12)	1.16 ± 0.17 (18)	0.80 ± 0.18 (5)	0.69 ± 0.19 (9)	0.50 ± 0.16 (13)
Retrograde velocity (μm/s)								
Size class								
Small	None	None	None	None	0.42 (1)	0.51 ± 0.18 (6)	None*	None*
Medium	None	None	None	None	0.56 (2)	0.39 ± 0.23 (7)	0.22 ± 0.17 (3)	0.54 ± 0.23 (9)
Large	None	None	None	None	None	0.17 (2)	0.17 ± 0.04 (5)	0.12 ± 0.03 (6)
All particles	None	None	None	None	0.51 ± 0.08 (3)	0.41 ± 0.23 (15)	0.19 ± 0.10 (8)	0.30 ± 0.22 (15)
Ratio of velocities orthograde/retrograde	—	—	—	—	2.27	1.95	3.6	1.67

All microtubules selected for analysis were part of the microtubule tangles (stage 4) and did not move vigorously, if they did change position (e.g., Fig. 5) this was taken into consideration and was not interpreted as a change of direction of particle movement. Microtubules of the A series are from one preparation to which 20 mM ATP had been added at the beginning. Microtubules of the B series are from a different preparation with an initial concentration of 5 mM ATP (the same preparation is depicted in Fig. 5). The total number of particles moving along individual microtubules was counted for a period of continuous observation (6 to 16 min). Frequency of movement in either direction was determined at intervals of 1 min (± SD). From these data the percentage of particles moving in the orthograde direction was derived; none means no such particles observed; numbers in parentheses are absolute numbers of orthograde particles. The exact orthograde and retrograde velocities were determined for ~20 representative particles on each microtubule. Here, none means no such particle was analyzed; although there may have been one or a few of this class observable. Since the velocity determination was performed using still frames on a television monitor, the analysis of the small particles in some preparations was not possible (\*none) due to their weak contrast on the monitor screen.



further translation but underwent a “fishtailing” deformation that consisted of a sequence of serpentine shapes (Fig. 7). In  $\sim 40$  such cases observed usually a certain segment of the front end of the microtubule was attached to the surface or otherwise immobilized (Fig. 8). Occasionally, such blocked microtubular segments freed themselves and underwent additional translation for many tens or hundreds of micrometers before encountering another obstacle. The fishtailing microtubular segment in Fig. 8 fractured when its radius of curvature became less than  $1 \mu\text{m}$ . Individual microtubules were followed over many microscope fields for up to 5 min. During this time they traveled far from the residual axoplasm without conspicuous diminution of their length or speed. The speed of the microtubules was independent of their length (Fig. 9).

It is striking that the movement of microtubules, including the serpentine movements, took place in a layer of fluid  $\sim 0.3 \mu\text{m}$  thick above the glass surface (as measured with the calibrated stage height adjustment of the microscope). This movement therefore can be considered to take place in an almost two-dimensional space. Only in a very few cases observed was part of a microtubule out of focus. However, in a few cases fishtailing of filaments descending from free suspension down to the surface layer was observed when they hit the surface, while the tail end was still out of focus. In these cases fishtailing was not maintained for an extended time, but the bent microtubules underwent elastic straightening, settled as stiff rods, and started gliding over the surface.

We should mention that even in fields where dozens of microtubule fragments are gliding over the glass there is little or no detectable interference between them when their paths cross. Even if particles remained attached to the front end of the microtubules no disturbance of the paths of the microtubules gliding over one another was detectable. Of a few hundred cases only one collision was observed where a microtubule with a particle attached deformed another microtubule which was struck “amidships.” This particle moved forward along the second microtubule up to its end while dragging the adhering microtubule along. In another case, one microtubule caused a second to bend at an angle of  $\sim 5^\circ$  when one moved over or under the tail end of the second.

We observed  $\sim 10$  microtubules that had been bent into a U shape or into rings (as if the ends were tied together by an invisible filament). These microtubules showed rotation in the plane of the focus on the surface of the cover glass (Fig. 10). This movement was again not disturbed by other microtubules passing through the area, and it appeared that these rings were rotating while loosely attached to the glass. Some showed a circling motion for several minutes.

The administration of the microtubule-stabilizing agent

FIGURE 5 A sequence of videomicrographs shows the interactions between two native microtubules (a and b) and two large particles (1 and 2), and bidirectional particle motion on microtubule B. Particles 1 and 2 move in the same direction along B; 1 migrates to the end of B but attaches transiently to A enough to deform it. A smaller particle in a (arrowhead) moves in the opposite direction of particles 1 and 2 on microtubule B and is just visible in frame b (arrowhead). Particle 2 makes dual contact with A and B in frames c and d, causing both A and B to deform due to the force applied by the particle to A and B. In frame e, the attachment of 2 to B is suddenly broken, but that of 2 to A remains. Both microtubules recoil elastically. Bar,  $2 \mu\text{m} \times 5,730$ .



TABLE II  
Velocity of Short Microtubule Segments Obtained by Homogenization

Type of preparation	MTs analyzed	MTs with head particles	Length $\mu\text{m}$	Velocity $\mu\text{m/s}$	Age of preparation while analyzed	Symbol in Fig. 9
					h	
Untreated cover glasses	17	0	$3.6 \pm 1.3$	$0.22 \pm 0.02$	0.25-1	●
Untreated cover glasses + taxol	19	2	$5.7 \pm 2.7$	$0.18 \pm 0.02$	2 -6.5	◆
Untreated cover glasses	20	9	$3.9 \pm 1.5$	$0.35 \pm 0.05$	0.25-1	■
Siliconized cover glasses	5	1	$5.1 \pm 1.6$	$0.35 \pm 0.08$	1 -1.5	▲
Siliconized cover glasses, preparation transferred to untreated cover glasses	20	5	$4.4 \pm 2.8$	$0.25 \pm 0.04$	2 -4	▼

MT, microtubule.

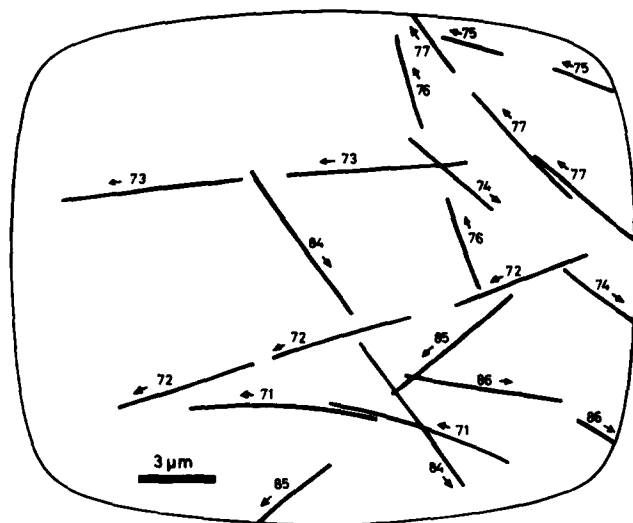


FIGURE 6 A population of native microtubule fragments obtained by shearing is observed in the presence of  $30 \mu\text{M}$  taxol for 5 min. Two or three positions are depicted at variable intervals for numbered microtubules, the velocities of which are given in Table II (taxol preparation). Note that the paths are almost but not quite straight, some deviating in either direction from straightness.

taxol (by replacement of the medium in the preparation three times with an equal volume of  $30 \mu\text{M}$  taxol-containing medium) did not interfere with particle transport or the gliding of microtubules (Table II and Fig. 11).

Modification of the glass surface by careful cleaning, siliconization, or treatment with poly-L-ornithine, poly-L-lysine, or poly-L-aspartate did not influence the gliding behavior of microtubular segments very much (Table II). Although the gliding microtubules appeared to be somewhat attracted by the surface of various kinds of differently treated cover glasses, on the hydrophobic siliconized glasses this "attachment" was more loose. In this case moving microtubules behaved like stiff rods continually undergoing small adjustments in direction although they never reversed their motile polarity (Fig. 6). More subtle differences may exist but must await further quantitative analysis.

As the preparations age and/or the concentration of ATP decreases, microtubule movement slows down (Table II) and an increasing number cease gliding.

#### Movements of Particles on Gliding Microtubules

Particles attached to and moved along short, gliding microtubules just as they did on longer segments in the tangled

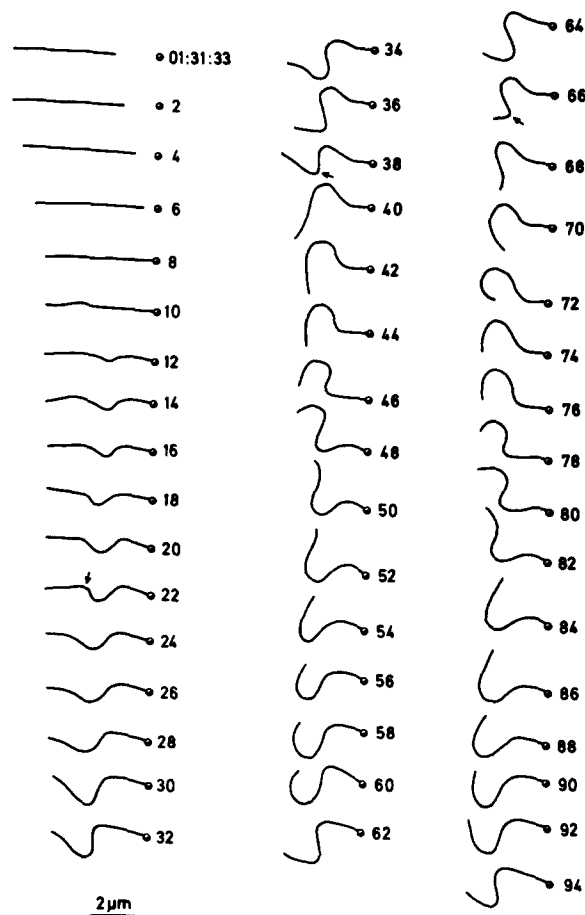
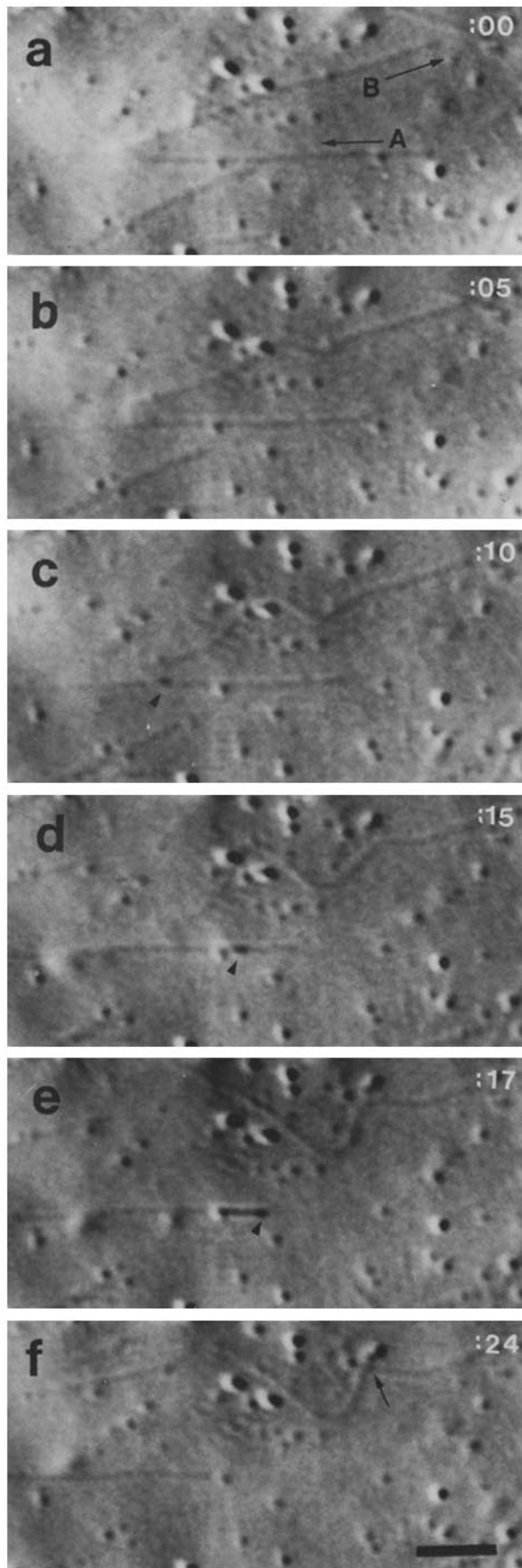


FIGURE 7 The sequence of straight and serpentine shapes assumed by a gliding microtubule before and after it encounters an obstacle. Times are in seconds. Left row shows arrival and initial bending of the microtubule. Center and right rows show a full cycle of 30 s. Arrows indicate maximal inflections that are the result of pushing forward on the part of the tail end of the microtubule. These shapes are followed by partial straightening of the microtubule due to elastic forces. The microtubule is  $4.8 \mu\text{m}$  long.

masses. Particles in some preparations traveled more frequently in the same (forward) direction in which the microtubules glided (Fig. 12). In most preparations, however, the particles moving in the direction opposite that of gliding were much more numerous. The velocity of microtubule gliding linearly correlates with the velocity of the particles moving backward simultaneously on the same microtubule (Fig. 13).

The organelles moving in the same direction as microtu-



bular gliding showed a very weak correlation coefficient, 0.44. We observed only four gliding microtubules that had bidirectional transport while gliding. In all of these cases, the velocities showed the same range and same relationship as those of microtubules attached to glass (See Table I, series B). The backward velocity was in all cases two to four times faster than the forward velocity (Table III), suggesting that the forward direction corresponds to the retrograde direction in Table I and in situ.

No difference was detected in the speeds of microtubule gliding in cases in which particles either did or did not move along them. When particles moved on microtubules partially attached to the surface and partially undergoing serpentine movement of the tail region, no conspicuous differences in speed could be observed when the particles passed from the waving tail to the immobilized front part or vice versa. Gliding microtubules that also transported particles often showed a particle stuck at the leading end (two examples are shown in Fig. 3). In some preparations almost all microtubules showed such particles. Particle movement and microtubule gliding slowed down as the preparations aged. In the stage at which most microtubules were already stuck to the surface, particle movement along stationary microtubules was still observed, although it occurred at a reduced speed.

#### Rotation of Microtubules on Their Axes

The manner of movement by both long and short microtubular segments suggested the possibility that this movement entailed rotation of the microtubule on its axis, as was suggested by Jarosch and Foissner (43). The present study neither confirmed nor excluded this possibility. That slightly bent ends of some microtubules protruding from tangles oscillated back and forth at  $\sim 1$  Hz, as if rotating slowly, favors this hypothesis.

If microtubules gliding over glass actually did rotate, one would expect lateral displacement of the microtubules during their translation. This is indeed the case for most of the

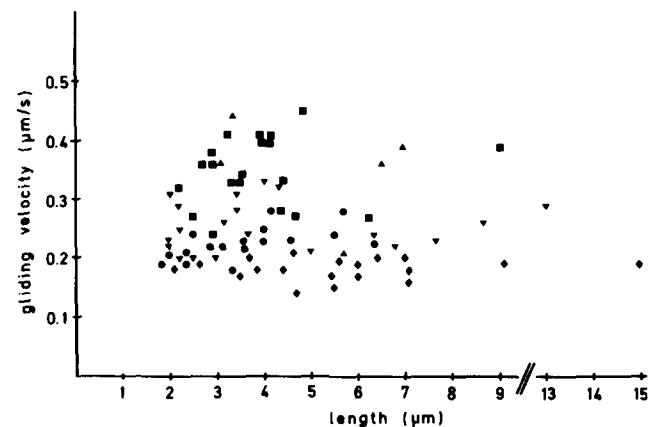


FIGURE 9 Gliding velocity is independent of microtubule length. For symbols see Table II.

FIGURE 8 A series of videomicrographs of two microtubules (A and B) initially gliding in opposite directions. A shows a small particle moving backward. B encounters an undetected obstacle or its front end becomes fixed to the glass. In b-e it becomes deformed into serpentine shapes. In f, it breaks into two fragments. Bar, 2  $\mu\text{m}$ .  $\times 6,000$ .

microtubules, but the lateral displacement is small (usually  $<0.5 \mu\text{m}$  per  $10 \mu\text{m}$  of movement). Since it occurs about equally often to the right- and to the left-hand side (there are several examples in Fig. 6), the data do not offer strong support for the rotation hypothesis.

The particles move equally well along filaments that appear to be either firmly attached to glass or are gliding freely. This suggests that their movement may not be helical around the microtubule.

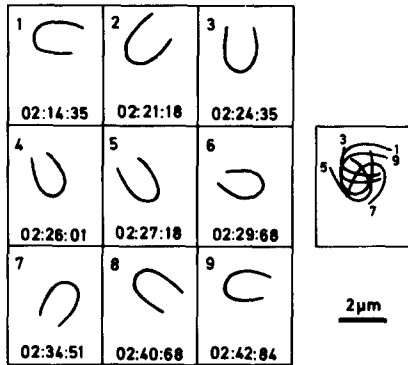


FIGURE 10 The rotation in the plane of focus of a U-shaped native microtubule. At the right is a composite image from the various times shown at the times indicated. Time is in minutes, seconds, and hundredths of a second. One full rotation is 28 s.

## DISCUSSION

### Interpretation of AVEC-Differential Interference Contrast Images

It has been shown previously that AVEC-differential interference contrast and AVEC-polarization microscopy can detect cytoskeletal and vesicular structures an order of magnitude smaller than the resolution limit of the microscope (3-5, 7, 8). However, it must be kept in mind that structures smaller than an Airy unit ( $\sim 0.2 \mu\text{m}$ ) are inflated to that size so that they may be imaged at some multiple of their physical size (4).

A possible limitation of video-enhanced microscopy suggested by this fact is that one may not always be able to discriminate between single, double, or multiple elements. Thus, it is significant that negatively stained preparations showed almost all of the microtubules to be single. It is interesting, however, that when two microtubules do lie in the same microdomain in one part of their length and diverge elsewhere, the contrast is doubled when they lie within the same microdomain or Airy disk diameter. Thus, one can actually discriminate single and paired microtubules on the basis of their image contrast even when they cannot be resolved.

The impression of particles riding on microtubules, although confirmed by electron microscopy (Fig. 4), does not prove their physical contact, since they might be separated by as much as 100 nm on either side of the microtubule.

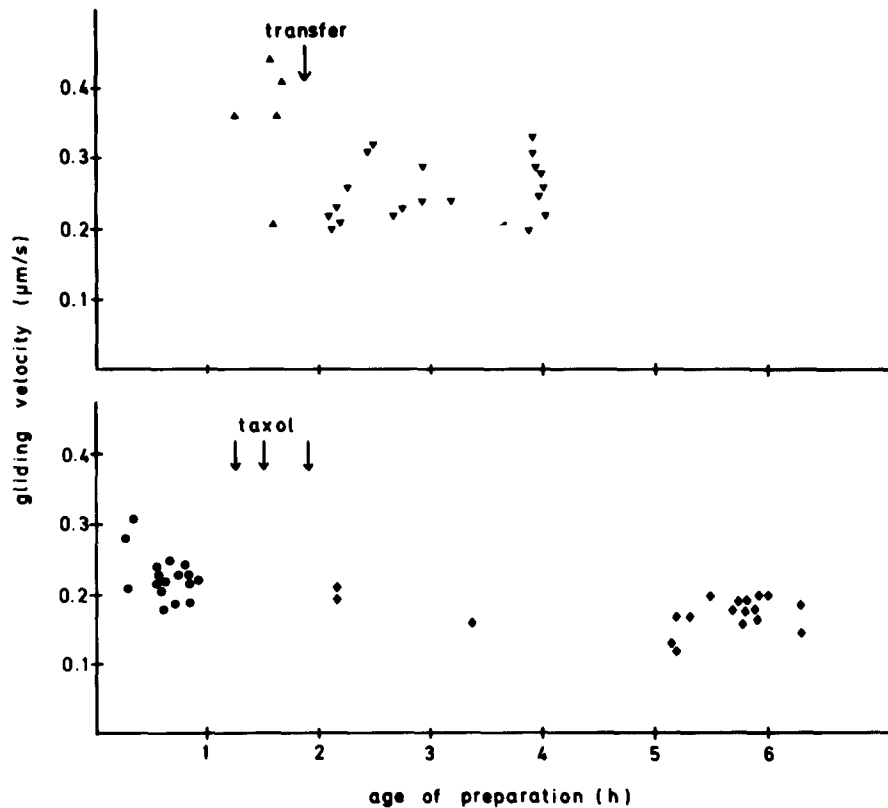
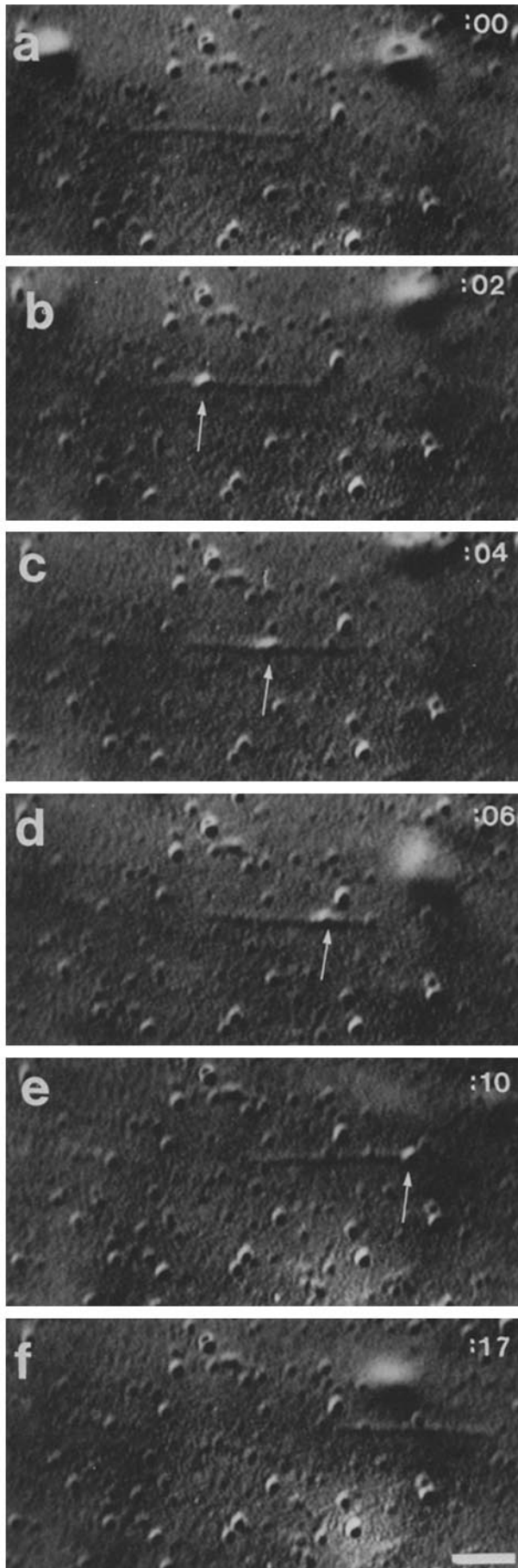


FIGURE 11 The velocity of microtubule gliding as a function of the age of the preparation. (Top) Removal of preparation from siliconized glass and transferred to untreated cover glass caused little or no change. (Bottom) Exchanging the medium of the preparation three times with  $30 \mu\text{M}$  taxol had no effect on the velocity. Preparations become slower with age. For symbols see Table II.



Although the viscoelasticity of squid axoplasm suggests cross-linking of the microtubules and other elements of the cytoskeletal scaffold, it is clear that such cross-linkage is lost during preparation or is so weak that it permits the microtubules to be so easily separated from this scaffold (compare references 45 and 56).

### *Unidirectional and Bidirectional Particle Transport*

It has been shown that cytoplasmic transport traffic occurs in contact with microtubules in frog keratocytes (35). Moreover, bidirectional particle transport, including movements of the same particles in both directions, occurs on single microtubules (6, 34). The live observations of transport were carried out by AVEC-differential interference contrast microscopy followed by whole-mount electron microscopy of the same preparations to confirm that transport occurred on a single microtubule. Similar findings have been reported on a microtubule from squid axoplasm (60).

From the polarized orientation of microtubules in neurons (19, 24, 36) and bidirectional traffic in intact axons and extruded axoplasm, one might expect that isolated native axonal microtubules would transport particles bidirectionally. However, contrary to this expectation, single microtubules in our preparations transported particles rapidly and unidirectionally in freshly made preparations and more slowly and bidirectionally when allowed to stand (Table I).

At present we cannot distinguish between two possibilities, (a) that the decrease of the orthograde speed due to a decrease in ATP concentration would permit more particles to move in a retrograde direction, and (b) that the decrease in the frequency of particles moving past any fixed point itself allowed retrograde movements to occur. The data in Table I are consistent with both possibilities, since in fast microtubules the large organelles are conveyed in the orthograde direction as well, and in slow microtubules they move predominantly in the retrograde direction. It is also possible that with time either the particles or the microtubules are modified so as to increase the frequency of bidirectional transport.

### *Microtubular Movement*

It was suspected earlier (6) that long microtubules themselves might be moving. Since there are no markers along these microtubules, the only way we could confirm this suspicion was to show that curved sectors of loop arcs changed in diameter. This is confirmed and substantiated in our report. We could also show that protruding microtubules (stage 3) and microtubules captured by one end in a tangle (stage 4) show bending and serpentine movements that are ATP dependent.

By causing the breakage of these long microtubules by shear, it was shown that segments 1.0 to 30  $\mu\text{m}$  long could glide along glass surfaces, even when the glass had been treated chemically in a variety of ways. This gliding movement is also ATP dependent (compare references 1 and 51) and insensitive to taxol at 30  $\mu\text{M}$ . Therefore, the movement would appear to

FIGURE 12 A 5  $\mu\text{m}$ -microtubule segment moves from left to right at the times shown (in seconds), and a particle alights (arrows) and moves forward to the end, where it is released. Bar, 2  $\mu\text{m}$ .  $\times 4,940$ .

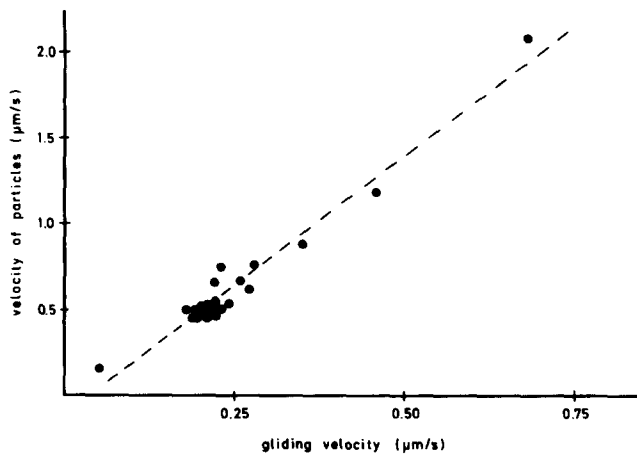


FIGURE 13 The backward velocities of particles relative to the microtubules are plotted against the gliding velocity of the same microtubule. The slope is 3.02, the  $y$ -intercept is  $-0.11$ , and  $r$  is 0.98. The forward velocities of particles (data not included) show a very weak correlation with slope = 2.19,  $y$ -intercept =  $-0.02$ , and  $r = 0.44$ .

be due to a mechanoenzyme, an ATPase, and not to treadmilling (47). The mechanism of this movement appears to reside on the microtubule itself or with some protein bound to native microtubules.

Except for our experiment involving the use of  $30 \mu\text{M}$  taxol (Table II and Fig. 6) which establishes that treadmilling is not necessary for gliding or axonal transport to occur, the gliding of microtubular segments has not yet been studied after various pharmacological treatments. However, it may be reasonable to rely on the pharmacology of the extruded axoplasm paradigm (16) and microinjected or permeabilized axons (26, 28) for a preliminary assessment of a likely mechanism for microtubule-associated transport. The pharmacology at present supports a central role for microtubules, and inhibition by erythro-9-[3-(2-hydroxy-nonyl)]adenine and vanadate is consistent with the involvement of a dynein or dynein-like mechanoenzyme although the definitive proof of such involvement is still missing. It is not yet clear, however, whether the available pharmacological data from the extruded axoplasm paradigm apply to particle transport alone or to microtubular gliding as well.

The close correlation of the speed of gliding with that of backward particle transport (Fig. 13) at the same time strongly supports the view that both motile phenomena are the result of the same force-generating mechanism.

The translatory movements of microtubular segments are unidirectional and therefore probably related to the growth polarity of the microtubule. Further details can be deduced from a comparison of the speeds of particles on microtubules attached to glass (Table I) with the speeds of particles on gliding microtubules (Table III). Since the movement of particles on these segments is predominantly backward, it is reasonable to suggest that this corresponds to the orthograde direction of transport in the intact axon. The forward transport of particles is less frequent, slower (Table III B), more variable in speed (Fig. 13), and therefore (by comparison with Table I) is assumed to correspond to retrograde transport. From these findings we conclude that the direction of microtubule gliding would correspond to the retrograde direction in situ. This was one of the predictions of the microstream hypothesis (72, 73).

Since the fast growing (+) end of microtubules is oriented toward the synapse (17, 24, 36), it seems probable that microtubules glide with their slow growing (–) ends forward.

The finding that vesicles often remain at the ends of gliding microtubules corresponds nicely with reports that in intact neurons numerous vesicles are often seen associated with microtubule ends (56).

### Possible Mechanoenzymes and Their Location

It has been shown by others that exogenous, inert particles are transported in axoplasm (2) and in other cells (11). This would appear to rule out a particle-associated mechanoenzyme unless the cytoplasm contains an excess of that enzyme with a specific affinity for the surface of particles transported. Certainly the transport of exogenous particles and gliding movement of microtubules in our preparations appear inconsistent with the idea that particle transport could result from a chemiosmotic gradient across particle membranes as was recently proposed (64).

Furthermore, the various forms of motility of microtubular segments clearly demonstrate that some mechanoenzymatic process occurs at or near the surface of the microtubule and exerts a force pushing towards the front end.

Since the microtubules are native, i.e., not reassembled from purified tubulin and microtubule-associated proteins, there may be mechanoenzymes associated with them. The fact that microtubular motility runs down without ATP and can be restored and accelerated by exogenous ATP strongly implicates an ATPase mechanoenzyme similar to either myosin or dynein. Such mechanoenzymes either have been reported in axons (for review see reference 71) or pharmaco-

TABLE III  
Speed of Particles Moving along Gliding Microtubules

	Speed $\mu\text{m/s}$		
A. Particles from different microtubules			
Gliding microtubules	$0.26 \pm 0.11$ (33)		
Forward particles relative to surroundings	$0.95 \pm 0.36$ (9)		
Backward particles relative to surroundings	$0.39 \pm 0.24$ (24)		
Forward particles relative to microtubule <sup>‡</sup>	$0.65 \pm 0.34$ (9)		
Backward particles relative to microtubule <sup>‡</sup>	$0.63 \pm 0.35$ (24)		
B. Particles from bidirectional microtubules <sup>‡</sup>			
	Backward	Forward	Ratio
Microtubule 1	0.70	0.18	3.89
2	1.13	0.36	3.14
3	1.21	0.71	1.70
4	0.64	0.24	2.67

<sup>\*</sup> Each microtubule showed only one particle, moving either backward or forward. Values are averaged from three different preparations. Forward and backward speeds cannot be compared because of the use of different microtubules. The total number of particles measured is given in parentheses.

<sup>‡</sup> These speeds are correlated with the speed of microtubule gliding.

<sup>‡</sup> These speeds are correlated with the speed of microtubule gliding as shown in Fig. 13.

<sup>‡</sup> The microtubules used each had one forward and one backward particle. Forward and backward speeds can be compared directly because they are measured from particles on the same microtubule. Speeds of particles are relative to the microtubule.

logical data showing sensitivity to vanadate and erythro-9-[3-2-(hydroxynonyl)]adenine have been interpreted as compatible with the behavior of a dynein-like molecule as an essential part of the mechanism of fast axonal transport (16, 25, 26, 28). Perhaps other mechanoenzymes remain to be discovered. The microtubule itself has long been known to turn over ATP, a process that has an unknown function (49, 53).

Ultrastructural data so far do not help in identifying any known mechanoenzyme such as myosin or dynein. Electron micrographs of negatively stained native microtubules show either smooth surfaces or the presence of a loose, amorphous (or possibly helical) fuzz around them (Fig. 4), or particles attached to microtubules by bridging filaments (66). On the other hand, observations in freeze-fracture preparations have been interpreted to mean that organelles are not connected to microtubules (59). It is likely that chemical fixation and dehydration may have removed or rendered unrecognizable any labile mechanoenzyme associated with the native microtubule. The image of native microtubules (Fig. 4) is certainly more complex than that of purified microtubules (45).

### *Molecular Models to Explain Microtubular Motility and Fast Axonal Transport*

The new findings can now be compared with the various possible mechanisms and some new possibilities can be discussed. Any valid theoretical approach must take into account a number of known facts derived from earlier works and the present study (for review see references 51, 70, and 71, and Table IV in reference 73):

(a) In intact axons, the speeds of orthograde and retrograde transport are about equal (7).

(b) Vesicles are transported continuously in one direction or the other without interruption; larger organelles move discontinuously in both directions (7) but predominantly in the retrograde direction. Although the speed of orthograde transport is similar for the various organelles, there are considerable differences in speed of retrograde particles.

(c) The orthograde and retrograde transport systems are specific for different types of particles in the intact nerve (23, 68, 71, 73).

(d) Particles move in both directions along microtubules attached to glass.

(e) Large and small particles can move in opposite directions along single microtubules, yet they very seldom collide or influence one another's speeds.

(f) Particles moving along one microtubule toward the junction with another can switch to the intersecting microtubule and move in either direction.

(g) Particles have more than one attachment site to the transport mechanisms (48).

(h) Gliding microtubules transport particles in both directions at similar speeds relative to the microtubule. The speed of backward movement is closely correlated with the speed of gliding, whereas with forward movement it is only weakly correlated.

(i) Even in microtubules that transport particles in both directions, asymmetry of movement is maintained, since the two directions differ in speed, particle transport frequency and size.

(j) Exogenous particles are also transported.

(k) Attached microtubules show ATP-dependent bending and undulation.

(l) Free microtubule segments move over glass surfaces at about one-quarter the speed of particles, apparently independent of the chemical nature of the surface. The direction of gliding probably corresponds to the retrograde direction in situ.

(m) At obstacles, microtubules continue to push toward their front end, performing serpentine movements.

(n) Gliding or fishtailing microtubules move over one another without mutual interference.

(o) Microtubule assembly-disassembly seems not to be involved in any of the above phenomena.

The formulation of any model must also take into account the following physical constraints and their consequences:

(i) The viscosity of the environment of native microtubules must be not far from that of water (1 centipoise [cP]) (32, 71, 73). For this reason, Brownian motion by suspended organelles and vesicles is so intense that it is difficult to follow the path of unattached particles from one television field (1/60 s) to the next.

(ii) The dimensions of microtubules and particles are so small that the Reynolds number characteristic of any flow in the system is vanishingly small ( $\sim 10^{-7}$ ). Consequently, any flow is laminar, and anything observed to move in a continuous manner must be acted upon continuously by the motive force. In other words, particles of this size can not coast if an instantaneous force gives them a brief kick (33, 54).

Taken together these facts and physical constraints would seem to call for a transport mechanism that operates with the particles bound to the microtubules, where they would be protected from the interference of continuous Brownian bombardment.

Given the apparent simplicity of microtubule structure (9, 21), we can consider how a rod- or paddle-shaped mechanoenzyme might operate to explain the known facts within the physical constraints of aqueous or cytoplasmic environments.

Microtubules might have on them evenly spaced mechanoenzyme molecules that could undergo a cycle of rotation or shape change as proposed for myosin (40, 65) or dynein (57). The mechanoenzymes could be positioned in either linear or spiral rows. Linear might be more likely, because particles apparently do not move spirally along microtubules (from fact *d*). The mechanoenzymes might have either a planar or an elliptical beat. If it were planar, two opposite power strokes would be required, and particles would be expected to collide and bump one another off the system (fact *e*). Two sets of oppositely oriented mechanoenzymes with a planar beat would also suffice, but then the forces would neutralize, and one would not expect the microtubule to glide, let alone glide while transporting particles (facts *h* and *l*).

If, however, the microtubule possessed a surface matrix of parallel mechanoenzyme molecules exhibiting coordinated elliptical cycles, then this would account for particle motions in both directions with little or no interference (fact *e*) at similar speeds (fact *h*).

Let us assume that during the middle of the orthograde portion of the beat cycle, the orientation of the mechanoenzyme is an extension of the microtubule radius, while in the middle of the retrograde cycle it is roughly tangential to the microtubule surface. Under those circumstances the retrograde traffic would be closer to the microtubule surface than the orthograde traffic, and two lanes would be established that would occupy different radial domains of the microtubules' circumtubular space and thus not mutually interfere (fact *e*).



The inclination of the orbits of the distal tip of the mechanoenzyme would place one of the lanes of traffic farther from the microtubule surface than the other. The coordinated movements of the mechanoenzyme tips with or without transported particles might create some local "microstreams" in both directions (65, 71, 73). The more distal stream away from the surface of the native microtubule would correspond to the orthograde direction and have the greatest effect upon the substratum (fact *l*), causing the microtubule to glide in the retrograde direction while particles would be transported in both directions at similar velocities in the two directions relative to the microtubule (fact *h*).

It is clear that some of the selectivity of the orthograde and retrograde transport mechanisms to the intact axon (23, 68) may be lost in some native microtubules (fact *f*). It is possible that selectivity may depend on the chemical nature or a charge distribution on particles, factors that could be altered when the cell is disrupted. Nevertheless, the asymmetry of the two transport systems (fact *i*) suggests that selectivity at least in part is a property of the native microtubule, which can even carry exogenous particles (fact *j*; compare references 2 and 11).

Any mechanism proposed to explain continuous motion along a microtubule (7, 31, 72, 73) in terms of microtubule-associated mechanoenzyme molecules must assume cooperativity of some kind among these molecules. Shimizu (65) has developed a theory of dynamic cooperativity of molecular processes in muscle contraction and myosin- and ATP-induced streaming along actin filaments in streaming chambers, which may be fundamentally applicable to other organized motile processes in cells. The starting point for his theory was the question raised by Schrödinger (61) about the applicability of equilibrium thermodynamics to living systems in which biological order would seem to demand nonequilibrium thermodynamics to account for cooperativity phenomena. Shimizu argues (reference 65, pp 228–232) that in muscle, cooperativity requires a metachronal rotation of myosin heads in conjunction with local streaming along the filaments. If you reasoned along the same lines, our hypothetical mechanoenzyme cycle could create a detailed model for a mechanically coupled, solid state transport system capable of conveying vesicles continuously in one direction while larger organelles would be transported continuously for some distance in the opposite direction. However, organelles that largely move in a retrograde direction often change speed or pause for varying periods, as if sometimes able either to respond to Brownian motion or ride the vesicle transport system.

If the hypothetical model for the functional native microtubule is extrapolated back to the intact axon, where the microtubule is only slowly, if at all, transported (14, 46, 69, 71), the gliding is no longer seen and organelles and vesicles are expected to operate as they do (facts *a* and *b*).

### *The Impact of Microtubular Motility on Other Models of Fast Axonal Transport*

It is interesting to note that the microstream hypothesis (31, 72, 73) predicts that isolated microtubules should glide in the retrograde direction on the basis of the proposal that a longitudinal stream is produced on their surfaces. The hypothesis was proposed that the mechanism of axonal transport is not regulated but free running whether particles are present or not (70). Furthermore, this hypothesis suggested that the flow

might be produced by ATP-dependent conformational changes of a microtubule-associated mechanoenzyme or by electro-osmosis, but it did not predict simultaneous bidirectional particle motion on a single microtubule. The new model proposed in this paper specifies one way in which streaming in both directions along restricted sectors of a microtubule could be produced; in that sense it is a microstream hypothesis, except that the microstream would be the result of mechanochemical transducers transporting particles in a solid state system. In the original theory, the transport of particles in the microstreams assumes that forces that maintain the particle in the stream are present and so strong that Brownian bombardment would not interfere. So far we do not know what such a force could be. If a further biophysical analysis of the movement showed that such attraction would be possible, by electrostatic or hydrodynamic forces, for example, then the scenario of the original microstream hypothesis would become acceptable (31, 73). Bidirectional flow is also reported to occur at various distances from the surfaces of swimming microorganisms (75). Much remains to be learned from a quantitative treatment of the phenomenon that would take into account the laws of hydrodynamics at very low Reynolds numbers (33, 54).

The facts that microtubules glide on glass and can transport exogenous and chemically inert molecules do not favor any model or theory that places the motive force on the particle itself. Thus, we can discard the hypothesis that the particles have transducer mechanoenzyme molecules on their surfaces that interact with microtubules in the manner proposed for myosin-coated particle movement along F-actin in the subcortical fibrils and endoplasmic filaments in *Nitella* cells. Myosin-coated covaspheres will move along F-actin cables of *Nitella* cortices (63) but will not move on squid axoplasmic native microtubules (Sheetz, M. P., R. D. Vale, and R. D. Allen, unpublished observations).

It has also been suggested that an actin–myosin interaction could play a central role in axonal transport (for review see reference 71). The results presented here seem to decrease further the likelihood that such a mechanism could be operating. At least we could not explain microtubular motility in terms of microtubule-associated actin thin filaments that we and others have been unable to demonstrate ultrastructurally. The data that support a role for actin involvement (reviewed in references 17 and 62) seem to require another explanation, perhaps in terms of the possible nonspecificity of inhibitors, or, in the case of gelsolin inhibition (17), possibly a mechanical interference due to the fragmentation of actin.

One hypothesis that can now be discarded is that Ca<sup>++</sup>-dependent contractions of the microtrabecular lattice might provide the force for axonal transport (22, 52, 67).

### *The Possible Significance of Microtubular Motility for Understanding Other Microtubule-dependent Transport Processes*

Microtubules are cytoskeletal elements that are almost ubiquitous in eucaryotic cells (21, 58). The fundamental processes of mitosis, meiosis, pronuclear transport leading to syngamy, intracellular transport associated with endocytosis, exocytosis and membrane processing, saltatory movements of organelles (55), the motions of pigment granules in some chromatophores, and the motile events associated with reticulopodial motility and feeding in foraminifera, radiolaria,

suctorians, and some other protists all fall in the category of microtubule-dependent movements because they are associated with the presence of oriented microtubules and are inhibited by such specific microtubule inhibitors as colchicine, vinblastine, and nocodazol (21, 58, 71).

A feature shared by all of these processes is the lack of a known, demonstrable motive force-generating mechanism, although in many cases inhibitor experiments are consistent with the presence of a hypothetical dynein-like mechanoenzyme, as has been suggested also for fast axonal transport (12, 25, 26, 28, 39; compare reference 71). However, Buckley and Stewart (18) found vanadate ineffective in halting saltations in cells in which the same concentration inhibits ciliary movement.

The demonstration that native microtubules from squid axoplasm can glide and simultaneously transport particles provides evidence for a testable general model that could explain some or all of the diverse microtubule-dependent motile and transport processes. The model for the general case is simple: if microtubules were anchored in or by the cytoskeleton, they could transport nuclei, cytoplasmic organelles, and vesicles, as in saltatory particle movement (55) and cytoplasmic transport including pigment migration in chromatophores and nutritive transport in protists (58). If microtubules were incompletely anchored or unanchored, they could themselves move and/or displace other microtubules or organelles. Such a mechanism could be an important component of the processes of mitosis and meiosis by providing the motive force for prometaphase and anaphase chromosomal transport, and could account for microtubular displacement as the mitotic apparatus changes form during mitosis. Such effects would be in addition to the well-known assembly and disassembly of microtubules during mitosis (10, 41).

The authors are grateful to Roger Sloboda, Guenter Gross, Hiroshi Shimizu, and Richard Weisenberg for valuable discussions. The help of Willi Maile in the quantitative evaluation of the data is gratefully acknowledged as is the excellent preparation of photographs by Kenneth Orndorff. We appreciated the loan of a video cassette recorder from Dr. Sloboda when ours broke down. Taxol was the generous gift of the Natural Products Branch of the National Institutes of Health. D. G. Weiss was supported by the Boehringer-Ingelheim Fonds. This project was supported by a grant (NS 19962) to Dr. Allen from the National Institute of Neurological and Communicative Disorders and Stroke. The microscope used was provided by a generous grant from the Rowland Foundation.

Received for publication 27 December 1984, and in revised form 19 February 1985.

*Note Added in Proof:* Since this paper was accepted, two articles (see below) appeared in *Cell* that contained results confirming some of our results presented here and in earlier publications (our references 6, 34, 35).

Work on the problem of the transport of organelles along microtubules began in our laboratory in 1982. We were pleased to have Michael Sheetz and Ronald Vale as guests in our laboratory for a short collaboration in August 1983. However, we are concerned that the literature published to date may have left some doubt as to the originality of our research and the priority of our respective discoveries. We raised this issue in a letter directed to Dr. Sheetz dated 7 June 1984. We received Dr. Sheetz' reply in his letter dated 12 June 1984, a portion of which we reproduce here:

We (Thomas S. Reese, Bruce J. Schnapp, Ronald D. Vale, and

Michael P. Sheetz) have always understood that you and your colleagues originally discovered vesicle movement on single filaments and we all make a point to acknowledge this both publicly and in private conversation. Like most major discoveries it will give birth to many derivative studies; we all feel obliged to ensure your original contribution not be forgotten.

We are gratified to have these researchers so unequivocally acknowledge the priority of our original work.

The two articles referred to above are: (a) Vale, R. D., B. J. Schnapp, T. S. Reese, and M. P. Sheetz. 1985. Movement of organelles along filaments dissociated from the axoplasm of the giant squid axon. *Cell*. 40:449-454. (b) Schnapp, B. J., R. D. Vale, M. P. Sheetz, and T. S. Reese. 1985. Single microtubules from squid axoplasm support bidirectional movement of organelles. *Cell*. 40:455-462.

## REFERENCES

- Adams, R. J. 1982. Organelle movement in axons depends on ATP. *Nature (Lond.)* 297:327-329.
- Adams, R. J., and D. Bray. 1983. Rapid transport of foreign particles microinjected into crab axons. *Nature (Lond.)* 303:718-720.
- Allen, R. D. 1985. New observations on cell architecture and dynamics by video-enhanced contrast optical microscopy. *Annu. Rev. Biophys. Biochem.* 14:265-290.
- Allen, R. A., and N. S. Allen. 1983. Video-enhanced microscopy with a computer frame memory. *J. Microsc.* 129:3-17.
- Allen, R. D., N. S. Allen, and J. L. Travis. 1981. Video-enhanced contrast, differential interference contrast (AVEC-DIC) microscopy: a new method capable of analyzing microtubule related motility in the reticulopodial network of *Allogromia laticollaris*. *Cell Motil.* 1:291-302.
- Allen, R. D., D. T. Brown, S. P. Gilbert, and H. Fujiwaka. 1983. Transport of vesicles along filaments dissociated from squid axoplasm. *Biol. Bull.* 165:523.
- Allen, R. D., J. Metzels, I. Tasaki, S. T. Brady, and S. P. Gilbert. 1982. Fast axonal transport in squid giant axon. *Science (Wash. DC)* 218:1127-1129.
- Allen, R. D., J. L. Travis, N. S. Allen, and H. Yilmaz. 1981. Video-enhanced contrast polarization (AVEC-POL) microscopy: a new method applied to the detection of birefringence in the motile reticulopodial network of *Allogromia laticollaris*. *Cell Motil.* 1:275-289.
- Amos, L. A. 1975. Substructure and symmetry of microtubules. In *Microtubules and Microtubule Inhibitors*. M. Borgers and M. DeBrabander, editors. Elsevier/North Holland Biomedical Press, Amsterdam. 21-34.
- Bajer, A. S., C. Cypher, J. Molé-Bajer, and H. M. Howard. 1982. Taxol-induced anaphase reversal: evidence that elongating microtubules can exert a pushing force in living cells. *Proc. Natl. Acad. Sci. USA* 79:6569-6573.
- Beckerle, M. C. 1984. Microinjected fluorescent polystyrene beads exhibit saltatory motion in tissue culture cells. *J. Cell Biol.* 98:2126-2132.
- Beckerle, M. C., and K. R. Porter. 1982. Inhibitors of dynein activity block intracellular transport in erythrocytes. *Nature (Lond.)* 295:701-703.
- Bear, T., F. Schmitt, and J. Z. Young. 1937. Investigations on the protein constituents of nerve axoplasm. *Proc. Roy. Soc. Lond. B. Biol. Sci.* 123:520-529.
- Black, M. M., and R. J. Lasek. 1980. Slow components of axonal transport: two cytoskeletal networks. *J. Cell Biol.* 86:616-623.
- Brady, S. T., R. J. Lasek, and R. D. Allen. 1982. Fast axonal transport on extruded axoplasm from squid giant axon. *Science (Wash. DC)* 218:1129-1131.
- Brady, S. T., R. J. Lasek, and R. D. Allen. 1985. Videomicroscopy of fast axonal transport in extruded axoplasm: a new model for study of molecular mechanisms. *Cell Motil.* 5:81-101.
- Brady, S., R. Lasek, R. D. Allen, H. Yin, and T. Stossell. 1984. Gelsolin inhibition of fast axonal transport indicates a requirement for microfilaments. *Nature (Lond.)* 310:56-58.
- Buckley, I., and M. Stewart. 1983. Ciliary but not saltatory movements are inhibited by vanadate microinjected into living cultured cells. *Cell Motil.* 3:167-184.
- Burton, P. R., and J. L. Paige. 1981. Polarity of axoplasmic microtubules in the olfactory nerve of the frog. *Proc. Natl. Acad. Sci. USA* 78:3269-3273.
- Collins, F. 1978. Axon initiation by ciliary neurons in culture. *Dev. Biol.* 65:50-54.
- Dustin, P. 1984. Microtubules. Second ed. Springer Verlag, Berlin. 1-480.
- Ellisman, M. H. 1982. A hypothesis for rapid axoplasmic transport based upon focal interactions between axonal membrane systems and the microtubular crossbridges of the axoplasmic matrix. In *Axoplasmic Transport*. D. G. Weiss editor. Springer-Verlag, Berlin. 390-396.
- Fahim, M., S. T. Brady, and R. Lasek. 1982. Axonal transport of membranous organelles in squid axons and axoplasm. *J. Cell Biol.* 95 (No. 2, Pt. 2):330a.
- Filliatreau, L. G., and L. Di Giambardino. 1981. Microtubule polarity in myelinated axons as studied after decoration with tubulin. *Biol. Cell.* 42:679-72.
- Forman, D. S. 1982. Vanadate inhibits saltatory organelle movement in a permeabilized cell model. *Exp. Cell Res.* 141:139-47.
- Forman, D. S., K. J. Brown, and D. R. Livengood. 1983. Fast axonal transport in permeabilized lobster giant axons is inhibited by Vanadate. *J. Neurosci.* 3:1279-1288.
- Gilbert, D. 1974. Physiological uses of the squid with special emphasis in the use of the giant axon. In *A Guide to the Laboratory Use of the Squid *Loligo pealei**. Marine Biological Laboratory, Woods Hole, MA. 45-55.
- Goldberg, D. J. 1982. Microinjection into an identified axon to study the mechanism of fast axonal transport. *Proc. Natl. Acad. Sci. USA* 79:4818-4822.
- Goldberg, D. J., D. A. Harris, B. W. Lubit, and J. A. Schwartz. 1980. Analysis of the mechanism of fast axonal transport by intracellular injection of potentially inhibitory molecules: evidence for a possible role of actin filaments. *Proc. Natl. Acad. Sci. USA* 77:7448-7452.
- Grafstein, B., and D. S. Forman. 1980. Intracellular transport in neurons. *Physiol. Rev.* 60:1167-1283.
- Gross, G. W. 1975. The microstream concept of axoplasmic and dendritic transport. *Adv. Neurol.* 12:183-196.

32. Gross, G. W., and D. G. Weiss. 1983. Intracellular transport in axonal microtubular domains. II. Velocity profile and energetics of circumtubular flow. *Protoplasma*. 114:198-209.
33. Happel, J., and H. Brenner. 1965. Low Reynolds number hydrodynamics. Prentice-Hall Inc., Englewood Cliffs. 1-553.
34. Hayden, J. H., and R. D. Allen. 1984. Detection of single microtubules in living cells: particle transport can occur in both directions along the same microtubule. *J. Cell Biol.* 99:1785-1793.
35. Hayden, J. H., R. D. Allen, and R. D. Goldman. 1983. Cytoplasmic transport in keratocytes: direct visualization of particle translocation along microtubules. *Cell Motil.* 3:1-19.
36. Heidemann, S. R., J. M. Landers, and M. A. Hamborg. 1981. Polarity orientation of axonal microtubules. *J. Cell Biol.* 91:661-665.
37. Heslop, J. P. 1974. Fast transport along nerves. *Soc. Exp. Biol. Symp. XXVIII.* 209-227.
38. Hodge, A. J., and W. J. Adelman. 1980. The neuroplasmic network in *Loligo* and *Hermisenda* neurons. *J. Ultrastruct. Res.* 70:220-241.
39. Hollenback, P. J., F. Suprynovicz, and W. Z. Cande. 1984. Cytoplasmic dynein-like ATPase cross-links microtubules in an ATP dependent manner. *J. Cell Biol.* 99:1251-1258.
40. Huxley, H. E. 1976. The relevance of studies on muscle to problems of cell motility. *Cold Spring Harbor Conf. Cell Prolif.* A:115-126.
41. Inoué, S. 1964. Organization and function of the mitotic spindle. In *Primitive Motile Systems in Cell Biology*. R. D. Allen and N. Kamiya, editors. Academic Press, Inc. NY. 549-594.
42. Isenberg, G. P., P. Schubert, G. W. Kreutzberg. 1980. Experimental approach to test the role of actin in axonal transport. *Brain Res.* 194:588-593.
43. Jarosch, R., and I. Foissner. 1982. A rotation model for microtubule and filament sliding. *Eur. J. Cell Biol.* 26:295-302.
44. Kerkut, G. A. 1975. Mini-review: axoplasmic transport. *Comp. Biochem. Physiol. A. Comp. Physiol.* 51:701-704.
45. Langford, G. M. 1983. Length and appearance of projections on neuronal microtubules in vitro after negative staining: evidence against a crosslinking function for MAPs. *J. Ultrastruct. Res.* 85:1-10.
46. Lasek, R. J., J. A. Garner, and S. T. Brady. 1984. Axonal transport of the cytoplasmic matrix. *J. Cell Biol.* 99 (No. 1, Pt. 2):212s-221s.
47. Margolis, R. L., and L. Wilson. 1981. Microtubule treadmills—possible molecular machinery. *Nature (Lond.)*, 293:705-712.
48. Martz, D., R. J. Lasek, S. T. Brady, and R. D. Allen. 1984. Mitochondrial motility in axons: membranous organelles may interact with the force generating system through multiple surface binding sites. *Cell Motil.* 4:89-101.
49. Murphy, D. B., R. R. Hiesch, and K. T. Wallis. 1983. Identity and origin of the ATPase activity associated with neuronal microtubules. I. The ATPase activity is associated with membrane vesicles. *J. Cell Biol.* 96:1298-1305.
50. Ochs, S. 1972. Fast transport of materials in mammalian nerve fibers. *Science (Wash. DC)*. 176:252-260.
51. Ochs, S. 1982. Axoplasmic transport and its relation to other nerve functions. John Wiley & Sons, NY.
52. Porter, K. R., H. R. Byers, and M. H. Ellisman. 1979. The cytoskeleton. In *The Neurosciences, Fourth Study Program*. F. O. Schmitt and F. G. Worden editors. MIT Press, Cambridge, MA. 703-722.
53. Prus, K., and M. Wallin. 1982. Microtubule-associated ATP-ase: fact or artifact? In *Axoplasmic Transport*. D. G. Weiss editor. Springer-Verlag, Berlin. 91-98.
54. Purcell, E. M. 1977. Life at low Reynolds number. *Am. J. Physiol.* 45:3-11.
55. Rebhun, L. I. 1972. Polarized intracellular particle transport: saltatory movements and cytoplasmic streaming. *Int. Rev. Cytol.* 32:93-137.
56. Sasaki, S., J. K. Stevens, and N. Bodick. 1983. Serial reconstruction of microtubular arrays within dendrites of the cat retinal ganglion cell: the cytoskeleton of a vertebrate dendrite. *Brain Res.* 259:193-206.
57. Satir, P., J. Wais-Steider, S. Lebduska, A. Nasr, and J. Avolio. 1981. The mechanochemical cycle of the dynein arm. *Cell Motil.* 1:303-327.
58. Schliwa, M. 1984. Mechanisms of intracellular organelle transport. In *Cell and Muscle Motility*. J. W. Shay editor, Raven Press, New York. 5:1-82.
59. Schnapp, B. J., and T. S. Reese. 1982. Cytoplasmic structure in rapid-frozen axons. *J. Cell Biol.* 94:667-679.
60. Schnapp, B., R. Vail, M. Sheetz, and T. S. Reese. 1984. Directed movements of organelles along filaments dissociated from squid giant axon. *Cell Biol. (Tokyo)*. 132a. (Abstr.).
61. Schrödinger, E. 1945. *What is Life?* Cambridge University Press, Cambridge. 1-91.
62. Schwartz, J. H. 1979. Axonal transport: components mechanisms and specificity. *Annu. Rev. Neurosci.* 2:467-504.
63. Sheetz, M. P., and J. A. Spudich. 1983. Movement of myosin-coated fluorescent beads on actin cables *in vitro*. *Nature (Lond.)*. 303:31-35.
64. Sheetz, M. P., B. J. Schnapp, R. D. Vale, and T. S. Reese. 1984. Organelle transport in squid axoplasm: inhibition by drugs that collapse proton gradients. *J. Cell Biol.* 99 (No. 4, Pt. 2):118a.
65. Shimizu, H. 1979. Dynamic cooperativity of molecular processes in active streaming muscle contraction, and subcellular dynamics. *Adv. Biophys.* 13:195-278.
66. Smith, D. S., U. Järlfors, and R. Beranek. 1970. The organization of synaptic axoplasm in the lamprey (*Petromyzon marinus*) central nervous system. *J. Cell Biol.* 46:199-219.
67. Stearns, M. E. 1980. Lattice-dependent regulation of axonal transport by calcium ions. In *Microtubules and Microtubule Inhibitors*. M. DeBrabander and J. DeMey, editors. Elsevier/North Holland Biomedical Press, Amsterdam. 17-30.
68. Tsukita, S., and H. Ishikawa. 1980. The movement of membranous organelles in axons. Electron microscope identification of anterogradely and retrogradely transported organelles. *J. Cell Biol.* 84:513-530.
69. Tytell, M., M. M. Black, J. A. Garner, and R. J. Lasek. 1981. Axonal transport: each major rate component reflects the movement of distinct macromolecular complexes. *Science (Wash. DC)*. 214:179-181.
70. Weiss, D. G. 1982. General properties of axoplasmic transport. In *Axoplasmic Transport in Physiology and Pathology*. D. G. Weiss and A. Gorio editors. Springer-Verlag, Berlin. 1-14.
71. Weiss, D. G. 1985. The mechanism of axoplasmic transport. In *Axoplasmic Transport*. Z. Iqbal editor. CRC Press, Boca Raton, FL. In press.
72. Weiss, D. G., and G. W. Gross. 1982. The microstream hypothesis of axoplasmic transport: characteristics, predictions and compatibility with data. In *Axoplasmic Transport*. D. G. Weiss, editor. Springer-Verlag, Berlin. 362-383.
73. Weiss, D. G., and G. W. Gross. 1983. Intracellular transport in axonal microtubular domains I. Theoretical considerations on the essential properties of a force generating mechanism. *Protoplasma*. 114:179-197.
74. Wolosewick, J. J., and K. R. Porter. 1979. Microtubular lattice of the cytoplasmic ground substance. Artifact or reality? *J. Cell Biol.* 82:114-139.
75. Wu, T. Y. 1977. Hydrodynamics of swimming at low Reynolds numbers. *Fortschr. Zool.* 24:149-169.